Characteristics of Tropical Easterly Wave Pouches during Tropical Cyclone Formation

ZHUO WANG AND ISAAC HANKES

Department of Atmospheric Sciences, University of Illinois at Urbana–Champaign, Urbana, Illinois

(Manuscript received 20 August 2013, in final form 23 October 2013)

ABSTRACT

The pregenesis evolution of wave pouches was examined for 164 named tropical cyclones that originated from zonally propagating tropical easterly waves over the Atlantic during July–October 1989–2010 using the European Centre for Medium-Range Weather Forecasts (ECMWF) Interim Re-Analysis (ERA-Interim) and the Climate Prediction Center (CPC) morphing technique (CMORPH) precipitation. East of 60°W, most wave pouches (~80%) form at 700 hPa first, often extending down to 850 or 925 hPa off the coast of West Africa. By contrast, the majority of the wave pouches (~68%) over the west Atlantic (west of 60°W) form at 850 or 925 hPa first. Wave pouches become more vertically aligned approaching genesis. It was also found that vorticity at 925 hPa intensifies faster than that at 600 hPa. A warm-core structure forms at the meso-β scale near the pouch center prior to genesis but is less well defined at the meso-α pouch scale. The evolution of precipitation and the low-level convergence suggests that convection begins to organize near the pouch center about 1 day prior to genesis, along with the rapid intensification of vorticity in the inner pouch region. The composites derived from ERA-Interim show that the inner pouch region has higher specific humidity and equivalent potential temperature, especially in the middle troposphere within 1 day prior to genesis.

1. Introduction

The formation of tropical cyclones (TCs) has been regarded, until recently, as a fundamental mystery of the tropical atmosphere. This is partly due to the lack of in situ observations capturing tropical cyclone formation over the remote ocean, and partly due to the multiscale nature of tropical cyclogenesis. The recently proposed marsupial paradigm for tropical cyclone formation within tropical easterly waves provides a framework to examine the multiscale interaction involved in tropical cyclone formation (Dunkerton et al. 2009). Using high-resolution model simulations, Wang et al. (2010a,b) and Montgomery et al. (2010) showed that the recirculation region within the wave critical layer, or the so-called wave pouch, acts as the ''guiding hand'' for aggregation of convective-scale vorticity anomalies. Although the genesis time and the intensity of the proto-vortex depend on mesoscale processes and have limited predictability, the genesis location is largely controlled by the parent wave's critical layer (Wang et al. 2010b). Since global models can forecast synoptic-scale disturbances with reasonable skill, the track of the preferred genesis location (i.e., the wave pouch center) can be predicted using global model operational data (Wang et al. 2009). The forecasts of pouch tracks and evolution based on the marsupial paradigm have been used in some recent field experiments, including the Tropical Cyclone Structure-2008 (TCS-08; Elsberry and Harr 2008), Pre-Depression Investigation of Cloud-systems in the Tropics (PREDICT; Montgomery et al. 2012), and National Aeronautics and Space Administration's (NASA's) Genesis and Rapid Intensification Processes (GRIP) Field Experiment (Braun et al. 2013), to provide useful guidance on flight planning.

The thermodynamic structure of the wave pouch and its impacts on moist convection and tropical cyclone formation were examined by Wang (2012) through the analysis of a numerical model simulation and dropsonde data from the PREDICT field experiment. It was found that the meso-β area near the pouch center (or the inner pouch region) is characterized by high saturation fraction and a short incubation time scale, which are believed favorable for deep convection and genesis. The analysis of dropsonde data showed that the midlevel equivalent potential temperature (θ_e) increases significantly near the pouch center 1–2 days prior to genesis

Corresponding author address: Zhuo Wang, Department of Atmospheric Sciences, University of Illinois at Urbana–Champaign, 105 South Gregory St., Urbana, IL 61801.
E-mail: zhuowang@illinois.edu

DOI: 10.1175/MWR-D-13-00267.1

but changes little away from the pouch center, which may indicate convective organization and the impending TC genesis near the pouch center. The difference between the inner pouch and outer pouch region was also observed by Davis and Ahijevych (2013).

Wang (2012) was based on the numerical simulation of a single storm and the dropsonde data analysis of limited cases. The objective of this study is to examine the dynamic and thermodynamic evolution of wave pouches, especially the difference between the inner pouch region and the meso-α-scale wave pouch, with a much larger sample size (164 named tropical cyclones) using the European Centre for Medium-Range Weather Forecasts (ECMWF) Interim Re-Analysis (ERA-Interim) data and Climate Prediction Center (CPC) morphing technique (CMORPH) precipitation. The data and methodology are described in section 2, and the results are presented in section 3, followed by a brief summary and discussion in section 4.

2. Data and method

The ERA-Interim (Simmons et al. 2007) is the latest ECMWF global atmospheric reanalysis. It utilizes four-dimensional variational data assimilation (4DVAR) and provides a more realistic representation of the atmosphere in both space and time than earlier reanalysis datasets. The spatial resolution of the data is about 0.7°, which is marginal to study meso-β-scale structures, but as shown later, the data capture the statistically significant differences between the inner pouch region (meso β) and the pouch scale (meso α). The 3-hourly precipitation from the CMORPH dataset (Joyce et al. 2004), with spatial resolution of 0.25°, was used as a proxy for convection. The precipitation estimates were derived from low-orbiting satellite microwave observations exclusively, and motion vectors derived from geostationary satellite IR data were used to propagate precipitation features. For the ERA-Interim data, we used a ~1.4° square box (3 × 3 grid points) to represent the inner pouch region, and a ~4.2° square box (7 × 7 grid points) to represent the pouch scale; for the CMORPH data, we used a 1.5° square box (7 × 7 grid points) to represent the inner pouch region, and a 4° square box (17 × 17 grid points) to represent the pouch scale. All the boxes are centered at and moving with the propagating pouch centers at 700 hPa.

The TC genesis time and locations were obtained from the National Hurricane Center (NHC) best track data. The wave pouch center was determined by the intersection of the wave trough axis and the wave critical latitude. The phase speeds of precursor waves were derived from the linear regression of the bandpass-filtered (Doblas-Reyes and Déqué 1998) 700-hPa meridional wind, following Dunkerton et al. (2009). The wave pouch was then tracked at 700, 850, and 925 hPa backward in time from genesis to day −10 (10 days prior to genesis) as long as a well-defined wave pouch was present. We focus on the named tropical cyclones over the Atlantic in July–October 1989–2010. There were 255 named storms during this time period. After excluding 41 storms without well-defined zonal propagating signals in the Hovmöller diagrams, 1 subtropical cyclone, 22 tropical storms without a wave pouch at 700 hPa at genesis,[1] and 27 waves with meridional propagation speed larger than 3.0 m s^{-1}, we have 164 storms left. The statistical analyses in section 3 are based on the 164 storms.

3. Results

The pouch tracks at 700, 850, and 925 hPa are shown in Fig. 1a. Also shown is the axis of the 700-hPa easterly jet. Over the Atlantic main development region (MDR; 10°–20°N, 80°–20°W), most of the pouch tracks are located south of the long-term mean jet axis. Among the 164 storms, 41 pouches at 700 hPa can be tracked back east of 10°W, some of them extending as far as 10°E. In contrast, only 10 (2) pouch tracks at 850 (925) hPa are present east of 10°W, suggesting that most wave pouches over West Africa have a shallow structure confined to ~700 hPa. This can be attributed to the strong vertical shear in the lower troposphere over West Africa. A significant increase in the 850- and 925-hPa pouch track density near the coast suggests that wave pouches tend to develop a deep structure after moving over to the ocean, probably because of the coastal convection and a decrease in the vertical wind shear. A secondary wave track is discernible over West Africa north of the jet axis[2] (e.g., Carlson 1969; Burpee 1974; Nitta and Takayabu 1985; Pytharoulis and Thorncroft 1999). Wave pouches are confined below 850 hPa along this northern track, and they move southwestward off the coast merging with the southern wave track (e.g., Reed et al. 1988a; Thorncroft and Hodges 2001). Pouch tracks are also present north of the jet over the west Atlantic and the Gulf of Mexico. These tracks are generally shorter than those in the MDR region. Some of the pouches may be associated

[1] Some of the 22 storms have a wave pouch present at either 850 or 925 hPa at genesis. They are excluded because the wave evolution is examined following the 700-hPa pouch track.

[2] Note that Fig. 1a only shows northern waves that have a closed circulation in the wave's comoving frame of reference. Not all northern waves have a pouch.

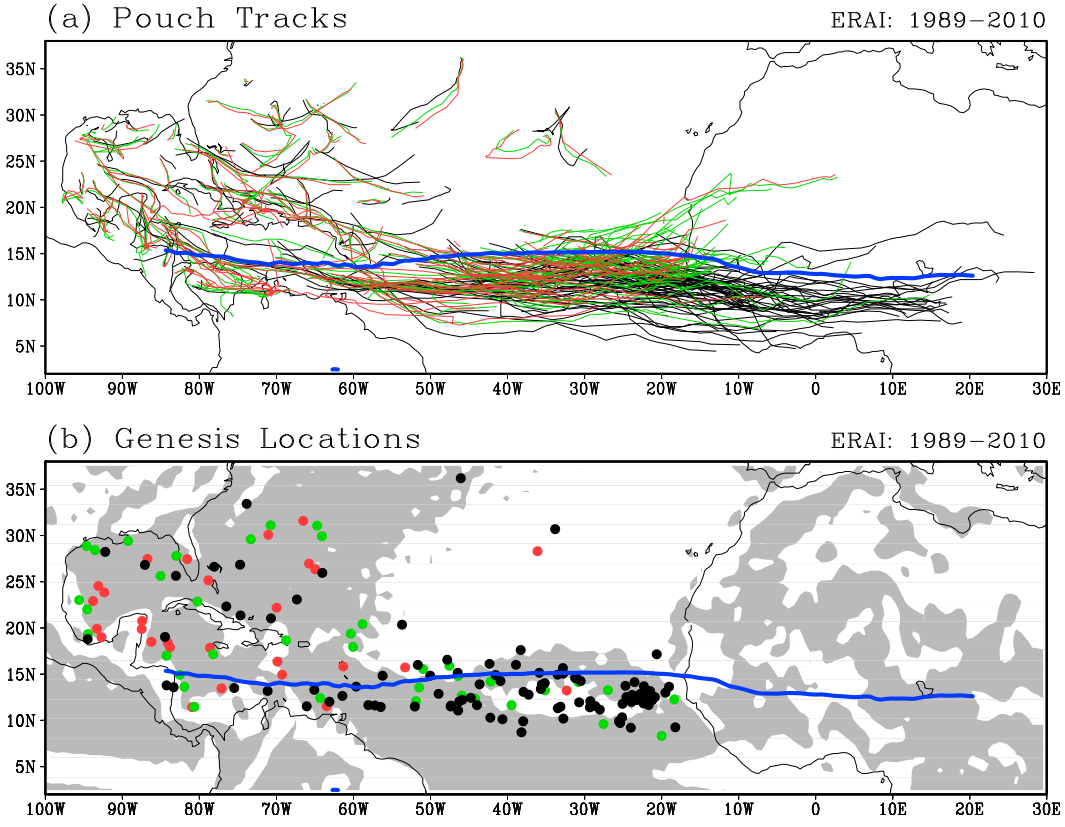

FIG. 1. (a) Wave pouch tracks at 700 (black), 850 (green), and 925 (red) hPa; (b) the TC genesis locations. Black, green, and red colors in (b) represent TCs that have a wave pouch first forming at 700, 850, and 925 hPa, respectively. Shading in (b) indicates regions of mean convergence at 850 hPa from the long-term mean during July–October 1989–2010. The thick blue curve represents the axis of the 700-hPa easterly jet from the long-term mean during July–October 1989–2010.

with wave disturbances forming over the Atlantic or associated with midlatitude frontal systems.

Tropical cyclogenesis locations are shown in Fig. 1b. Over West Africa, the east and central Atlantic (east of 60°W), most of the wave pouches (~80%) formed at 700 hPa first, while about 68% of tropical cyclones over the west Atlantic (west of 60°W) had a wave pouch forming at 925 or 850 hPa first. This is related to the zonal variations of the mean flow. Over West Africa and the east Atlantic, the mean flow is characterized by a well-defined, meridionally confined jet peaking at 600–700 hPa. The jet weakens westward and gradually transitions into a broad region of trade wind easterlies peaking at 850–900 hPa over the west Atlantic. Also shown in Fig. 1b is the long-term mean convergence at 850 hPa during July–October. Nearly all the tropical cyclones developed in a region of low-level convergence.

The distribution of wave pouch lifetime is shown in Fig. 2a. Among the 164 named storms, 97%, 90%, 82%, and 79% of them have a wave pouch form by 12 h prior to genesis at 700, 850, 925 hPa, and all of the three levels, respectively. In total, 32% of the storms have a pouch form at 700 hPa more than 5 days prior to genesis. Wang et al. (2012) suggested that a deep wave pouch extending from ~600 hPa down to the boundary layer is a highly favorable condition for genesis. Other factors that need to be considered for genesis include SST, vertical shear, etc. (e.g., Gray 1968).

The vertical displacement of the wave pouches with respect to 700 hPa, which is defined as the horizontal distance between the pouch centers at two levels, is examined in Fig. 2b. On average, there is a 1°–2° displacement within 3 days prior to genesis. The displacement has a general tendency of decreasing approaching the genesis time, which is consistent with the study by Dunkerton et al. (2009) using a smaller sample size. A vertically aligned wave pouch is believed to be a favorable condition for genesis (Wang et al. 2012; Raymond and López Carrillo 2011; Davis and Ahijevych 2012).

To examine the dynamic evolution of the wave pouch at different spatial scales, the 925- and 700-hPa relative

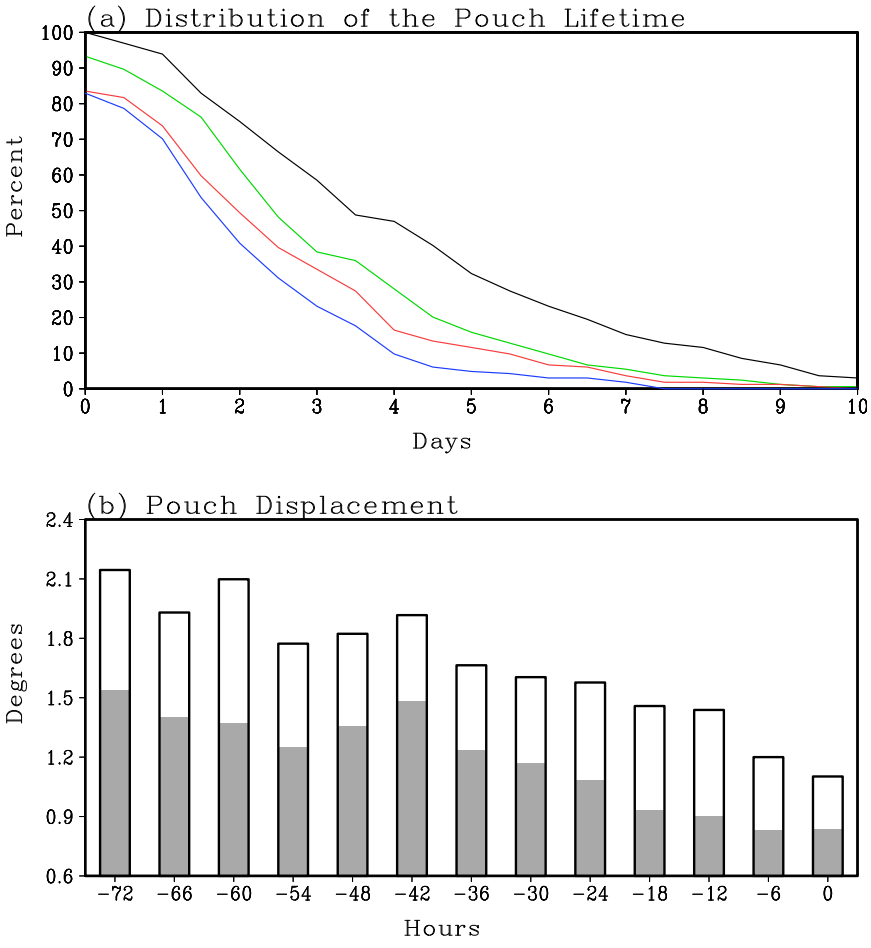

FIG. 2. (a) The percentages of waves with the pouch lifetime equal to or longer than the indicated time (the abscissa; units: days) at 700 hPa (black), 850 hPa (green), 925 hPa (red), and a deep pouch at all of the three levels (blue); $t = 0$ day indicates the percentages of waves having a pouch at genesis. (b) The mean displacement (units: degrees) of the 850-hPa (gray bars) and 925-hPa (open bars) wave pouch centers with respect to the 700-hPa pouch centers.

vorticity and the Okubo–Weiss parameter[3] (OW) averaged over the inner pouch region and the meso-α pouch scale are shown in Fig. 3. The difference between the inner pouch and the pouch-scale averages implies a difference between the inner and outer pouch regions. An evident feature in Figs. 3a,b is that the mean vorticity and OW in the inner pouch region are much stronger than those averaged over the pouch scale, suggesting that the inner pouch region is characterized by stronger rotation and weaker deformation compared to the outer pouch region. The averages over the inner pouch region and over the pouch scale both show stronger vorticity and OW at 700 than at 925 hPa at the early stage, which is consistent with the typical vertical structure of an African easterly wave (e.g., Reed et al. 1988b). However, because of a larger intensification rate at 925 hPa, the 925-hPa vorticity (and OW) exceeds that at 700 hPa 18 h prior to genesis in the inner pouch region, suggesting the formation of a warm-core structure at the meso-β scale. At the pouch scale, the relative vorticity at 925 hPa becomes close to but does not exceed that at 700 hPa, and a well-defined warm-core structure is absent even at genesis. The different vorticity evolutions at different spatial scales are consistent with the numerical model simulation in Wang (2012). Wang (2012) showed that vorticity evolves differently at different spatial scales: the spin up of the meso-β-scale low-level circulation near the pouch center precedes the spin up of the mid-level vortex, while at the meso-α pouch-scale vorticity

[3] The OW parameter is a measure of the "shape preserving" component of a vortical flow (Rozoff et al. 2006; Dunkerton et al. 2009) and is defined by $\mathrm{OW} = \zeta^2 - S_1^2 - S_2^2$, where ζ is relative vorticity and S_1 and S_2 represents the strain rate. Positive values of OW indicate that the flow is rotation dominant, and negative values of OW suggest that the flow is susceptible to rapid filamentation.

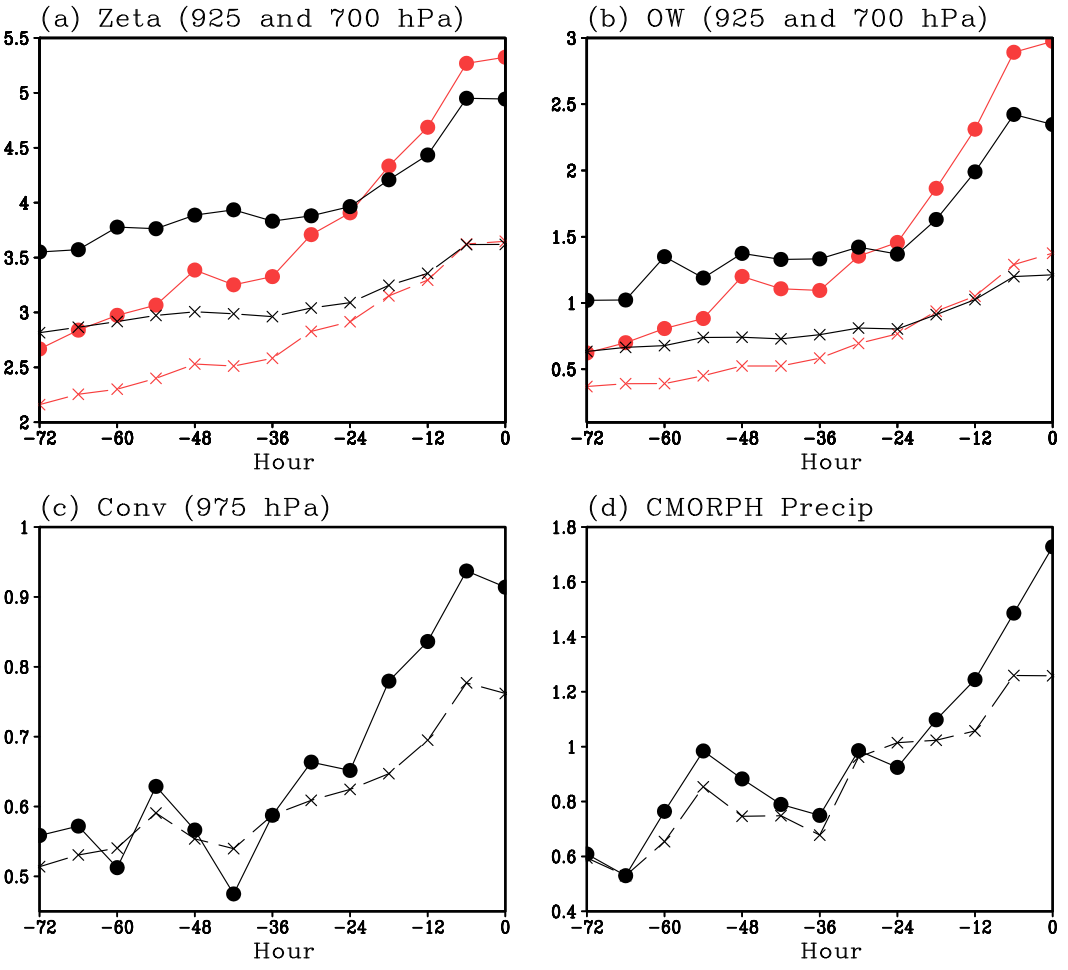

FIG. 3. Areal averages of (a) 925- (red curves) and 700-hPa (black curves) vorticity (units: $10^{-5}\,s^{-1}$), (b) 925- (red curves) and 700-hPa (black curves) OW (units: $10^{-9}\,s^{-2}$), and (c) 975-hPa convergence (units: $10^{-5}\,s^{-1}$) derived from ERA-Interim for 1989–2010; (d) precipitation rate ($mm\,h^{-1}$) derived from the CMORPH dataset for 2003–10. Multiplication signs represent averages over the pouch scale, and closed circles represent averages over the inner pouch area.

increases in the middle troposphere first. Wang (2012) attributed the different vorticity evolution to the different thermodynamic conditions in the inner and outer pouch regions and the resultant convective distribution.

Figure 3c shows the 975-hPa convergence averaged at the two different scales. At the early stage the two averages have large fluctuations and are close to each other. From $t = -30$ h onward, the convergence averaged over the inner pouch region exceeds that averaged at the pouch scale, indicating that convection has begun to organize near the pouch center. The time series of precipitation rate conveys the same message. Also notable in Fig. 3a is a larger intensification rate of relative vorticity within 24 h prior to genesis compared to the early stage. The rapid intensification in vorticity coincides with the significant increase in the low-level convergence and precipitation within ~24 h prior to genesis, and is consistent with an abrupt transition to strong deep convection shortly before genesis suggested by Wang (2013, manuscript submitted to *J. Atmos. Sci.*).

The thermodynamic condition of the wave pouch is examined in Fig. 4. The differences in specific humidity (SH), air temperature T, and θ_e between the inner pouch region and the pouch scale were calculated. The significance of the differences was examined in two Student's t tests. In the first test, the inner pouch average and the pouch-scale average of a storm are treated as a paired observation, and a one-sample one-sided t test is carried out with the null hypothesis that the difference between the inner pouch and the pouch-scale averages is zero. In the second test, the inner pouch averages and the pouch-scale averages are treated as independent

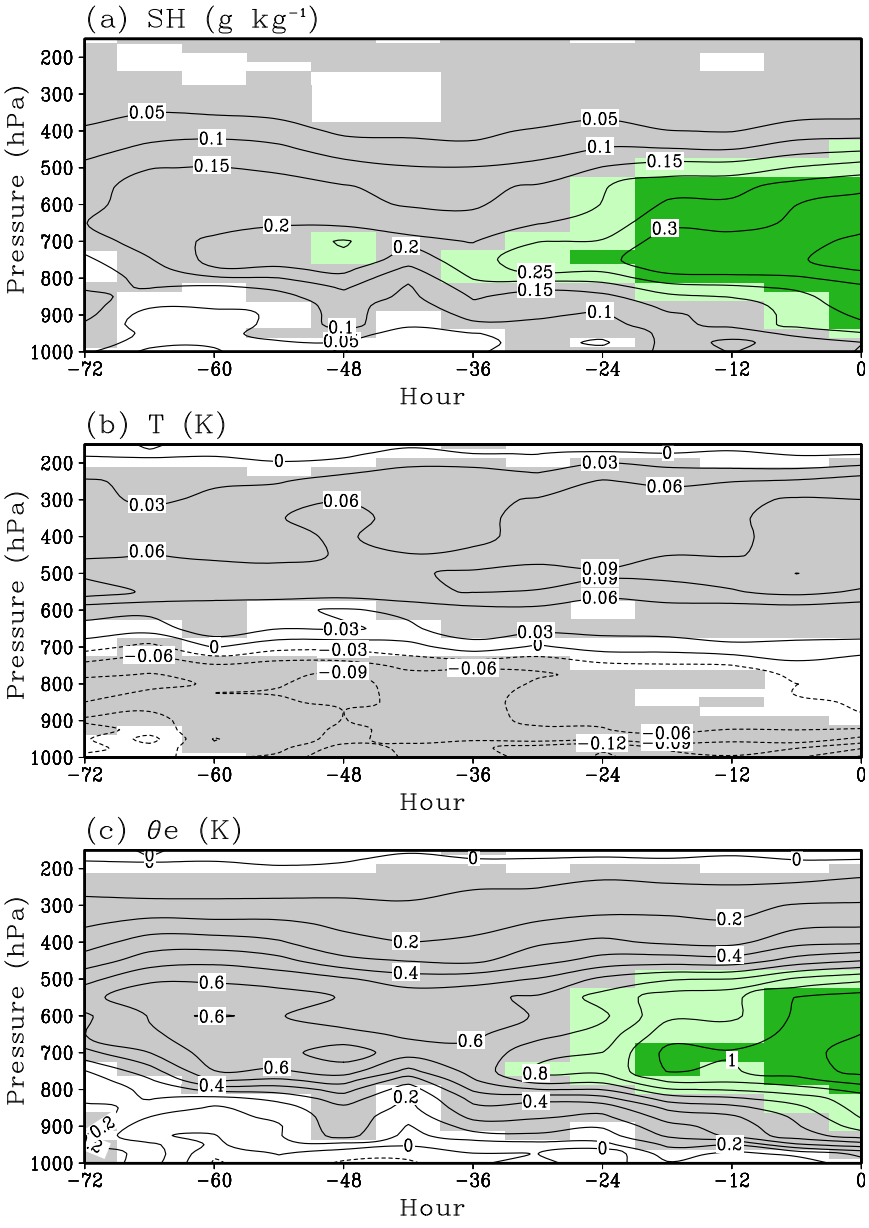

FIG. 4. Differences of (a) specific humidity (units: g kg^{-1}), (b) air temperature (units: K), and (c) equivalent potential temperature (units: K) between the inner pouch averages (~1.4°) and the pouch-scale averages (~4.2°) from 72 h prior to genesis to the genesis time. Gray shading highlights differences exceeding the 99% confidence level for paired samples, and light and dark green shadings highlight differences exceeding the 95% and 99% confidence levels for independent samples, respectively.

samples, and a two-sample one-sided t test is carried out with the null hypothesis that the inner pouch averages and the pouch-scale averages have the same sample means. The second test is stricter (or more sensitive) than the first test (Wilks 2006, chapter 5.2).

Figure 4a shows that the inner pouch has larger specific humidity than the pouch-scale average. The magnitude of the difference is very small ($\leq$0.2 g kg^{-1}), but it exceeds the 99% confidence level for paired samples at most vertical levels from $t = -72$ h to genesis, and exceeds the 99% (95%) confidence level for independent samples between 550 and 800 hPa within 18 (24) h before genesis. The higher water vapor content in the inner pouch region is consistent with the findings by Wang (2012) in a high-resolution numerical model simulation and dropsonde data analysis. Wang (2012)

suggested that the high moisture content in the inner pouch region is related to the dynamic and kinematic structure of the wave pouch and contributes to convective organization near the pouch center. Figure 4a is also consistent with Nolan (2007), who emphasized the importance of column moistening for tropical cyclogenesis.

Figure 4b shows that the inner pouch is relatively warmer than the pouch scale above 700 hPa and colder below. The difference exceeds the 99% confidence level for paired samples most of the time but does not exceed the 95% confidence level for independent samples. Significant cold anomalies in the lower troposphere become more confined near the surface within the 24 h prior to genesis. Despite the small magnitude (less than 0.1 K at most levels), the temperature difference is consistent with the transition of the circulation from a cold-core structure to a warm-core structure near the pouch center (Fig. 3a). The temperature difference also indicates enhanced static stability in the inner pouch region, which was also reported by Davis and Ahijevych (2013) in dropsonde data analysis. Raymond et al. (2011) suggested that a midlevel vortex with the associated enhanced static stability helps to create a more conducive environment for tropical cyclone formation by making the vertical mass flux profile of deep convection more bottom heavy. Although Fig. 4b indicates enhanced static stability in the inner pouch region, it is worth pointing out that the temperature difference is present more than 3 days prior to genesis and does not show a progressive increase as the moisture difference does. Besides being consistent with the vertical structure of the circulation, the significance of the temperature field and enhanced static stability to convection and genesis cannot be determined by the analysis here. Instead, the steady increase in midlevel moisture suggests the importance of midlevel moistening for tropical cyclone formation.

Figure 4c shows that the inner pouch region has higher θ_e than the pouch-scale average above the boundary layer. The difference maximizes around 700 hPa and exceeds the 99% (95%) confidence level for independent samples within 18 (24) h prior to genesis. Comparison between Figs. 4a and 4b suggests that the difference in θ_e mainly results from the humidity difference, which is consistent with Wang (2012). Given the spatial resolution of the ERA-Interim data, it is not a surprise that the magnitude of the difference is much smaller than that derived from dropsonde data.

4. Summary and discussion

The evolution of wave pouches prior to genesis was examined for 164 named tropical cyclones that originated from zonally propagating tropical easterly waves over the Atlantic during 1989–2010. It was found that most (~80%) wave pouches east of 60°W form at 700 hPa first. A wave pouch over West Africa is often confined to around 700 hPa, and tends to extend to 850 or 925 hPa off the coast of West Africa. Over the west Atlantic (east of 60°W), a larger fraction (68%) of wave pouches develop at either 850 or 925 hPa first. A wave pouch becomes more vertically aligned approaching genesis.

The evolution of vorticity and OW shows that the circulation at 925 hPa intensifies faster than that at 600 hPa. A warm-core structure develops at the meso-β scale near the pouch center prior to genesis, but a well-defined warm core structure is absent at the meso-α pouch scale. The comparison of precipitation and the low-level convergence evolution between the inner pouch region and the meso-α pouch scale suggests that convection becomes organized or concentrated near the pouch center about 1 day prior to genesis, which coincides with a rapid intensification in vorticity in the inner pouch region. The ERA-Interim composites also show significant moistening in the inner pouch region, especially in the middle troposphere within 1 day prior to genesis.

This statistical analysis of the ERA-Interim data revealed the different thermodynamic conditions and different vorticity evolution between the inner and outer pouch regions, and, along with the analysis of the CMORPH precipitation, suggests that the inner pouch region is the preferred location for sustained deep convection and tropical cyclogenesis, which supports the recent findings by Wang (2012) based on case studies. This study also shows that the ERA-Interim data can capture the mesoscale pouch structure to some extent. A more in-depth analysis of the wave structure and evolution using the ERA-Interim and satellite data is under way and will be reported in due course.

Acknowledgments. This research was supported by the National Science Foundation Grants ATM-1016095 and ATM-1118429. The ERA-Interim data were downloaded from the Research Data Archive at the National Center for Atmospheric Research, Computational and Information Systems Laboratory (NCAR CISL). We thank three anonymous reviewers for their constructive comments.

REFERENCES

Braun, S. A., and Coauthors, 2013: NASA's Genesis and Rapid Intensification Processes (GRIP) Field Experiment. *Bull. Amer. Meteor. Soc.,* **94,** 345–363.

Burpee, R. W., 1974: Characteristics of the North African easterly waves during the summers of 1968 and 1969. *J. Atmos. Sci.,* **31,** 1556–1570.

Carlson, T. N., 1969: Some remarks on African disturbances and their progress over the tropical Atlantic. *Mon. Wea. Rev.,* **97,** 716–726.

Davis, C. A., and D. A. Ahijevych, 2012: Mesoscale structural evolution of three tropical weather systems observed during PREDICT. *J. Atmos. Sci.,* **69,** 1284–1305.

——, and ——, 2013: Thermodynamic environments of deep convection in Atlantic tropical disturbances. *J. Atmos. Sci.,* **70,** 1912–1928.

Doblas-Reyes, F. J., and M. Déqué, 1998: A flexible bandpass filter design procedure applied to midlatitude intraseasonal variability. *Mon. Wea. Rev.,* **126,** 3326–3335.

Dunkerton, T. J., M. T. Montgomery, and Z. Wang, 2009: Tropical cyclogenesis in a tropical wave critical layer: Easterly waves. *Atmos. Chem. Phys.,* **9,** 5587–5646.

Elsberry, R. L., and P. A. Harr, 2008: Tropical cyclone structure (TCS-08) field experiment science basis, observational platforms, and strategy. *Asia-Pac. J. Atmos. Sci.,* **44,** 209–231.

Gray, W. M., 1968: Global view of the origin of tropical disturbances and storms. *Mon. Wea. Rev.,* **96,** 669–700.

Joyce, R. J., J. E. Janowiak, P. A. Arkin, and P. Xie, 2004: CMORPH: A method that produces global precipitation estimates from passive microwave and infrared data at high spatial and temporal resolution. *J. Hydrometeor.,* **5,** 487–503.

Montgomery, M. T., Z. Wang, and T. J. Dunkerton, 2010: Coarse, intermediate and high resolution numerical simulations of the transition of a tropical wave critical layer to a tropical storm. *Atmos. Chem. Phys.,* **10,** 10 803–10 827.

——, and Coauthors, 2012: The Pre-Depression Investigation of Cloud-Systems in the Tropics (PREDICT) Experiment: Scientific basis, new analysis tools, and some first results. *Bull. Amer. Meteor. Soc.,* **93,** 153–172.

Nitta, T., and Y. Takayabu, 1985: Global analysis of the lower tropospheric disturbances in the Tropics during the northern summer of the FGGE year. Part II: Regional characteristics of the disturbances. *Pure Appl. Geophys.,* **123,** 272–292.

Nolan, D. S., 2007: What is the trigger for tropical cyclogenesis? *Aust. Meteor. Mag.,* **56,** 241–266.

Pytharoulis, I., and C. Thorncroft, 1999: The low-level structure of African easterly waves in 1995. *Mon. Wea. Rev.,* **127,** 2266–2280.

Raymond, D. J., and C. López Carrillo, 2011: The vorticity budget of developing typhoon Nuri (2008). *Atmos. Chem. Phys.,* **11,** 147–163.

——, S. L. Sessions, and C. López Carrillo, 2011: Thermodynamics of tropical cyclogenesis in the northwest Pacific. *J. Geophys. Res.,* **116,** D18101, doi:10.1029/2011JD015624.

Reed, R. J., A. Hollingsworth, W. A. Heckley, and F. Delsol, 1988a: An evaluation of the ECMWF operational system in analyzing and forecasting easterly wave disturbances over Africa and the tropical Atlantic. *Mon. Wea. Rev.,* **116,** 824–865.

——, E. Klinker, and A. Hollingsworth, 1988b: The structure and characteristics of African easterly wave disturbances as determined from the ECMWF Operational Analysis/Forecast System. *Meteor. Atmos. Phys.,* **38,** 22–33.

Rozoff, C. M., W. H. Schubert, B. D. McNoldy, and J. P. Kossin, 2006: Rapid filamentation zones in intense tropical cyclones. *J. Atmos. Sci.,* **63,** 325–340.

Simmons, A., S. Uppala, D. Dee, and S. Kobayashi, 2007: ERA-Interim: New ECMWF reanalysis products from 1989 onwards. *ECMWF Newsletter,* No. 110, ECMWF, Reading, United Kingdom, 25–35.

Thorncroft, C., and K. Hodges, 2001: African easterly wave variability and its relationship to Atlantic tropical cyclone activity. *J. Climate,* **14,** 1166–1179.

Wang, Z., 2012: Thermodynamic aspects of tropical cyclone formation. *J. Atmos. Sci.,* **69,** 2433–2451.

——, M. T. Montgomery, and T. J. Dunkerton, 2009: A dynamically-based method for forecasting tropical cyclogenesis location in the Atlantic sector using global model products. *Geophys. Res. Lett.,* **36,** L03801, doi:10.1029/2008GL035586.

——, ——, and ——, 2010a: Genesis of Pre–Hurricane Felix (2007). Part I: The role of the easterly wave critical layer. *J. Atmos. Sci.,* **67,** 1711–1729.

——, ——, and ——, 2010b: Genesis of Pre–Hurricane Felix (2007). Part II: Warm core formation, precipitation evolution, and predictability. *J. Atmos. Sci.,* **67,** 1730–1744.

——, ——, and C. Fritz, 2012: A first look at the structure of the wave pouch during the 2009 PREDICT–GRIP dry runs over the Atlantic. *Mon. Wea. Rev.,* **140,** 1144–1163.

Wilks, D. S., 2006: *Statistical Methods in the Atmospheric Sciences.* 2nd ed. Academic Press, 648 pp.